Proceedings of the 17th World Congress
The International Federation of Automatic Control
Seoul, Korea, July 6-11, 2008

System Analysis of a Hybrid Two-component Development Process for Xerography

Feng Liu*, George T.-C. Chiu*
Eric S. Hamby, Yongsoon Eun****

**Purdue University, West Lafayette, IN 47907 USA*
(Tel: 765-294-2688; e-mail: liuf,gchiu@ purdue.edu)
***Xerox Corporation, Webster, NY 14580 USA*
(Tel: 585-422-4156; e-mail: Eric.Hamby,Yongsoon.Eun@xerox.com.

Abstract: In this paper, we will illustrate the utility of a control oriented model for a hybrid two component development process. More specifically, we will focus on the developability loss phenomenon observed in low throughput printings, where a monotonic increasing development voltage is required to achieve same amount of developed mass per unit area, which is highly correlated with the color appearance on the print images. For a given initial condition, the acceptable operating region for the development process is bounded by maximal and minimal toner mass levels as well as a maximal development voltage. We will demonstrate that the state trajectory will eventually leave the acceptable operating region in finite time for all continuous state feedback control involving dispensing input.

1. INTRODUCTION

Xerography is the "dry-marking" process used in majority of the laser printers and copiers. A typical xerographic process includes 6 sequential steps around a photoreceptor: 1) charging, 2) exposure, 3) development, 4) transfer, 5) fusing, and 6) cleaning as shown in Figure 1. During charging, a high-voltage corona or charge roller is used to induce a uniform layer of charges on the surface of the photoreceptor. Pulsed laser or LED light discharges (exposes) selected areas on the photoreceptor surface to form a latent charge image. During development, a bias voltage is applied between the photoreceptor and the development housing to generate an electrostatic field, which forces charged toner particles to move from the toner cartridge to the surface of the photoreceptor to form a toner image. During the transfer step, another electrostatic field is used to transfer the toner particles from the photoreceptor surface to a pre-charged media (e.g. paper). In fusing, heat and pressure is applied during the fusing process to permanently attach the melted toner particles to the media. Finally, residual toner particles on the photoreceptor surface are 'cleaned' off with help of a blade or a brush to prepare the photoreceptor surface for the next xerographic cycle. More detailed description of the xerographic process can be found in literatures (Shein 1988 and Pai *et al*., 1993). In this study, we only focus on the development process.

During development, the toner particles are subjected to mechanical stresses associated with rolling and impact contacts while being transported through a set of augers and rollers. Figure 2 shows the different surface geometries between a freshly dispensed (new) toner particle and one that has been in the development area for some time (aged toner particle). This change in surface geometry has been correlated to the loss of toner charge property (Ramesh 2005), which requires an increase in electrostatic field strength to transport the toner particles to the photoreceptor, commonly referred to as "developability loss". And the evolution of the toner property is referred to as the toner aging effect/dynamics. For low relative humidity and low area coverage print jobs, e.g. pages with only a few characters, only a small fraction of toner particles in the development area is developed onto the photoreceptor, while the rest remains and is subjected to repeated mechanical stresses. Under this type of "stress operating conditions", elevated development bias voltage is usually needed to maintain consistent amount of toner development (Li *et al*., 2001), i.e. color consistency. This practice eventually leads to saturation of the development bias voltage that results in inconsistent color reproduction from prints to prints over time.

In xerographic process, another actuator with easy access is the toner dispenser, since its motor speed can be adjusted to control the dispensing rate of developer materials (toners, carrier, *etc*.). It is easy to see that this actuator can only provide non-negative input, since materials can only not be subtracted from the developer housing. Due to practical limitations, it is also assumed that the dispenser input is continuous. With this extra actuator, the following question can be naturally raised: Is it possible to avoid saturating the bias voltage under low area coverage conditions with a "smart" dispensing strategy? In our previous work (Liu *et al*., 2006a, b), a control-oriented model was constructed based on a comprehensive phenomenological model (Ramesh 2005). Using the control oriented model, this paper presents the first analytical results that successfully predicted the loss of developability in a xerographic development process.

The remaining of this paper is organized as follows. In Section 2, the hybrid two-component development process and the control oriented model are briefly reviewed. In Section 3, we analyze the system dynamics to answer the

question proposed above. Concluding remarks are given in Section 4. A detailed proof of a theorem in Section 3 can be found in the appendix. A nomenclature list is also provided in Table 1 for quick reference.

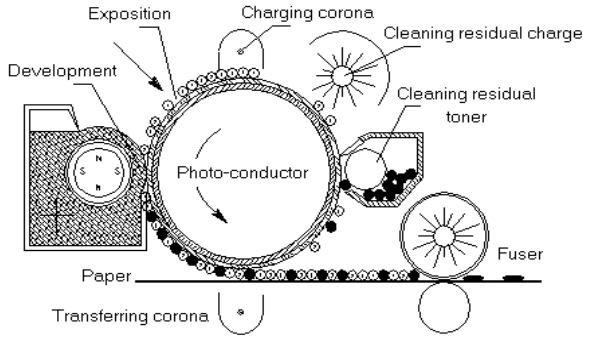

Fig. 1. Sequential steps of the xerographic process.

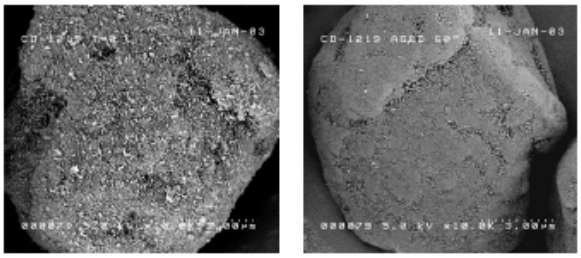

Fig. 2. Photomicrograph of fresh toner (left) and aged toner (right)

Table 1. Nomenclature

Symbols	
DMA	developed mass per unit area
DMA^*	target values of developed mass per unit area
TC	toner concentration in the sump
M_c	carrier mass (assumed constant)
$V_{dev}(t)$	development voltage
$V_{dev}^*(t)$	development voltage needed to achieve DMA^*
$D_t(t)$	dispensing rate
$C_t(t)$	throughput rate
$R_w(t)$	waste rate
M_d	toner mass on the donor roll (assumed constant)
$M_t(t)$	toner mass in the sump
$\gamma_s(t)$	sump state
$\gamma_d(t)$	donor state
$x(t)$	state vector
x_0	initial state
$u(t)$	control vector
p_a	fraction of free additives (material property)
λ	tracking gain between sump and donor state
γ_L	local slope of development curve around (V_{dev}^*, DMA^*)
Ω	acceptable operating region
W	admissible input set
T_f	operating time
T_f^{max}	maximal operating time
M^l	lower bound on toner mass
M^u	upper bound on toner mass
V^u	maximal allowable development voltage
X_{eq}	a superset of equilibrium state
Δ	projection of Ω on the M_t-γ_d phase plane

2. PROCESS DESCRIPTION AND CONTROL ORIENTED MODEL

2.1 Process Description

Figure 3 illustrates a hybrid two component development process (Liebman 1975 and Hirsch 2006), where uncharged toner and carrier particles are dispensed from the dispenser to the sump area. In the sump area, the toner and carrier particles are mixed and transported through a set of augers. The mixing enables tribo-charge between the particles and induces charges on the toner and carrier particles. Additives are also dispensed to control the charging process and the particle flow. The carrier particles attached with toner particles are attracted to a magnetic roller (Mag roll in Figure 3). The toner particles are then detached from the carrier particles and developed onto the donor roll. As the donor roller rotates and aligns with the development electrostatic field, the field strength detaches the charged toner particles and developed them onto the photoreceptor surface.

The developed mass per area (*DMA*) on the photoreceptor is a measure of the effectiveness of the development process. It has been shown to be highly correlated with the color appearance on the print image. As a result, it is desired to keep the *DMA* at a constant level under different operating conditions to maintain color consistency. In the sump area, toner concentration (*TC*), which is defined as the ratio of the toner mass M_t to that of the carrier mass M_c, i.e. M_t/M_c, is frequently used as an indicator of the charging status. In most processes, the carrier mass M_c can be assumed to be constant.

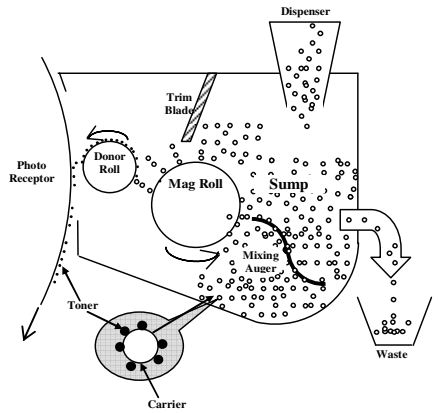

Fig. 3. Schematic of a hybrid two component development process

2.2 Control Oriented Model

In our previous work (Liu *et al.*, 2006a), the development process is modeled as a cascade structure of a static mapping and toner aging dynamics, which is characterized using three state variables as shown in Figure 4. The term $D_t(t)$ is the dispensing rate and $V_{dev}(t)$ is the development bias voltage, these two are the control inputs to the process (i.e. actuators). The term $C_t(t)+ R_w(t)$ is the effect of throughput and waste, which can be regarded as the disturbance input to this process. The output of the process is the *DMA* on the photoreceptor. To achieve constant *DMA*, active adjustment of the development voltage is usually required. This will partially compensate the toner aging effect, which is represented by γ_L in this model. The states are toner mass $M_t(t)$, sump state $\gamma_s(t)$

and donor state $\gamma_d(t)$, where the sump and donor states characterize the "goodness" of the toner at different locations in the system such that smaller values for these states correspond to reduced developability. The sump state and the donor state are scaled to take on values between 0 and 1, where 1 represents fresh toner. The evolution of the states $x(t)=[M_t(t),\ \gamma_s(t),\ \gamma_d(t)]^T$ with respect to the control inputs $u(t)=[D_t(t)\ ,V_{dev}(t)]^T$ can be summarized as following:

$$\dot{x}(t)=h(x(t),u_1(t))=\begin{bmatrix} u_1(t)-C_t(t)-R_w(t) \\ \frac{u_1(t)}{x_1(t)}(1+p_a)(1-x_2(t))-\beta\cdot x_2(t) \\ \frac{u_1(t)p_a}{x_1(t)}(1-x_3(t))+\lambda\frac{C_t}{M_d}(x_2(t)-x_3(t))-\beta x_2(t) \end{bmatrix}, \quad (1)$$

where p_a and β are parameters related to developer material properties, M_d is the estimated (constant) toner mass on the donor roll, λ is a model parameter identified from experiments or more complicated numerical models. The sump state and donor state are both in the range of [0, 1]. The output *DMA* is approximated around its target value DMA^*:

$$DMA\approx DMA^*+\gamma_L\cdot(V_{dev}-V_{dev}^*):=f_1(\gamma_L,V_{dev},DMA^*,V_{dev}^*)\ . \quad (2)$$

where V_{dev}^* is the development bias voltage needed to achieve DMA^* and γ_L is the local slope. Experimental data suggest that γ_L can be modeled as a monotonic increasing function of the following variables: the toner mass in the development area M_t, the relative humidity RH (assumed to be constant in this research), and the developability of toner particles on the donor roller γ_d, and V_{dev}^* can be modelled as a decreasing function with respect to γ_d, i.e.

$$\begin{aligned}\gamma_L&=f_2(M_t,RH,\gamma_d)\\ V_{dev}^*&=f_3(M_t,RH,\gamma_d)\end{aligned}\ . \quad (3)$$

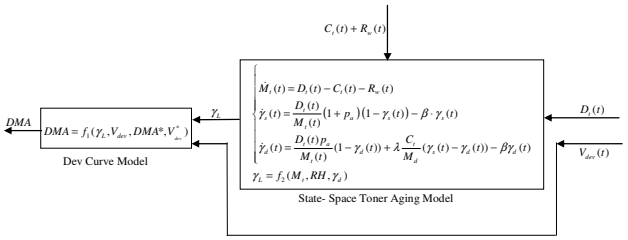

Fig. 4. Block diagram of the control oriented model

3. SYSTEM ANALYSIS

In this section, the control oriented model reviewed in Section 2 will be analyzed to explain certain experimental observations. More specifically, we will focus on the developability loss phenomenon observed in low throughput printing and try to answer the question proposed in the introduction, i.e. is it possible to avoid saturating the bias voltage under low area coverage conditions with a "smart" dispensing strategy? For a given initial condition, the acceptable operating region for the development process is bounded by maximum toner mass levels as well as maximum development voltage. We will demonstrate that the state trajectory of (1) will eventually leave the acceptable operating region in finite time for all continuous state feedback control involving the dispensing input, D_t. Noting that although the system has two control inputs $u=[D_t\ ,V_{dev}]^T$, only D_t has control authority on the toner aging dynamics, while V_{dev} only effects the output *DMA*.

Before diving into detailed analysis, several concepts need to be defined. For a system defined in (1)-(3), an *acceptable operating region* Ω is defined as a *compact* subset of the state space such that the desired output *DMA* can be maintained while keeping the input V_{dev} and state M_t within their maximum and minimum bounds, i.e.

$$\begin{aligned}&\Omega(M^l,M^u,V^u)\\ &:=\{(M_t,\gamma_s,\gamma_d)\,|\,M^l\le M_t\le M^u,V_{dev}^*(M_t,\gamma_d,RH)\le V^u\}\end{aligned}\ , \quad (4)$$

where M^l and M^u denote the lower and upper bound for the state M_t respectively. V^u denotes the maximal allowable control input. Using (3), the last condition in the above definition can be written into bounds on state γ_d, i.e.

$$V_{dev}^*(M_t,\gamma_d,RH)\le V^u\ \ \Rightarrow\ \ \gamma_d\ge\gamma_{\min}(M_t,V^u,RH)\ , \quad (5)$$

where γ_{min} is the lower bound of γ_d for the state trajectory to stay within the acceptable operating region. Therefore, an acceptable operating region Ω can be redefined as

$$\begin{aligned}&\Omega(M^l,M^u,V^u)\\ &:=\left\{(M_t,\gamma_s,\gamma_d)\,\middle|\,\begin{matrix}0\le\gamma_s\le1,0\le\gamma_d\le1\\ M^l\le M_t\le M^u,\gamma_d\ge\gamma_{\min}(M_t,V^u,RH)\end{matrix}\right\},\end{aligned} \quad (6)$$

as shown in Figure 5. With Ω defined by (6), if we define an initial state $x_0:=x(t)|_{t=0}$, the corresponding *operating time* T_f can be defined as

$$\begin{aligned}&T_f(M^l,M^u,V^u,x_0,D_t)\\ &:=\inf\left[t\ge0\,\middle|\,x_0\in\Omega(M^l,M^u,V^u),x(t)\notin\Omega(M^l,M^u,V^u)\right]\\ &=\inf\left[t\ge0\,\middle|\,\begin{matrix}x_0\in\Omega(M^l,M^u,V^u)\\ M_t(t)\notin[M_t^l,M_t^u]\text{ or }\gamma_d(t)<\gamma_{\min}(M_t(t),V_{dev}^u,RH)\end{matrix}\right]\end{aligned}\ . \quad (7)$$

where Ω is defined in (6) and the system dynamics is defined in (1). In other words, T_f is the time the state trajectory leaves Ω, the acceptable operating region for the first time. Given (M^l,M^u,V^u) and a fixed initial condition x_0, the maximal operating time T_f^{max} can be defined as

$$\begin{aligned}&T_f^{\max}(M^l,M^u,V^u,x_0):=\sup_{D_t(t)\in W}\left[T_f(M^l,M^u,V^u,x_0,D_t)\right]\\ &=\sup_{D_t(t)\in W}\left\{\inf\left[t\ge0\,\middle|\,\begin{matrix}x_0\in\Omega\\ M_t(t)\notin[M_t^l,M_t^u]\text{ or }\gamma_d(t)<\gamma_{\min}(M_t(t),V_{dev}^u,RH)\end{matrix}\right]\right\}.\end{aligned} \quad (8)$$

where W is the set of all admissible dispensing inputs. In this research, W is assumed to be the set of all non-negative state feedback based control law, which is also continuous, i.e.

$$W:=\left\{D_t(t)\,\middle|\,D_t(t)\ge0\text{ and }D_t(t)=g(x),\text{ i.e. state feedback control}\right\}.$$

The non-negative requirement above is from the fact that dispenser can only add more materials into the system, while the continuous requirement is due to the practical limitation of actuators, which also guarantees that the resulting closed-loop system can still be represented by continuous ordinary differential equations.

To show that the state trajectory of (1) will eventually leave the acceptable operating region, it is equivalent to show that $T_f^{max}<\infty$. For future reference, we also define T_s^{max} as

$$\begin{aligned}&T_s^{\max}(M^l,M^u,V^u,x_0)\\ &:=\sup_{D_t\in W}\left\{\inf\left[t\ge0\,\middle|\,\begin{matrix}x_0\in\Omega\\ M_t(t)\notin[M_t^l,M_t^u]\text{ or }\gamma_s(t)<\gamma_{\min}(M_t(t),V_{dev}^u,RH)\end{matrix}\right]\right\}.\end{aligned} \quad (9)$$

It is worth noting that the difference between T_f^{max} and T_s^{max} is that the bound is on γ_d in (8) and on γ_s in (9).

In system analysis, a subset M of the state space is said to be *positively invariant* with respect to the system dynamics, if $x_0 \in M$, $x(t) \in M$, for all $t \geq 0$ (Khalil 2002). A subset Q of the state space is said to be *controlled invariant* with respect to the system dynamics, if there exists a continuous feedback control which assures the existence and uniqueness of the solution of the closed-loop system and it is such that Q is positively invariant (Blanchini 1999, Nijmeijer *et al.*, 1982). For the development process dynamics modeled in (1), we have the following invariant property.

Claim 1: The set $\{(M_t, \gamma_s, \gamma_d) \mid 0 \leq \gamma_d \leq \gamma_s \leq 1\}$ is controlled invariant for any positive dispensing $D_t(t) \geq 0$.

Proof:

This can be shown using the vector field of (1) at the boundary as shown in Figure 10.

At the boundary of the set, we have

at (0, 0) $0 \leq \dot{\gamma}_d = \dfrac{D_t(t)}{M_t(t)} p_a < \dfrac{D_t(t)}{M_t(t)}(1+p_a) = \dot{\gamma}_s$,

at (1, 0) $\dot{\gamma}_d = \dfrac{D_t(t)}{M_t(t)} p_a + \lambda \dfrac{C_t(t)}{M_d} \geq 0 \qquad \dot{\gamma}_s(t) = -\beta < 0$,

at (1, 1) $\dot{\gamma}_d = \dot{\gamma}_s = -\beta$,

at $\gamma_d = 0$ $\dot{\gamma}_d = \dfrac{D_t(t)}{M_t(t)} p_a + \lambda \dfrac{C_t(t)}{M_d} \gamma_s > 0$,

at $\gamma_d = 1$ $\dot{\gamma}_s(t) = -\beta < 0$,

at $\gamma_d = \gamma_s$ $\dot{\gamma}_s - \dot{\gamma}_d = \dfrac{D_t(t)}{M_t(t)}(1-\gamma_s) \geq 0$.

These results indicate that at the boundary of the set, the state trajectory points inside of the set, and this is true for all possible $D_t(t) \geq 0$.

Remark 1: In practice, since all printers start with the initial condition $\gamma_d(0) = \gamma_s(0)$, this claim guarantees $\gamma_d(t) \leq \gamma_s(t)$ for any $t \geq 0$. Referring to the definitions of T_f^{max} and T_s^{max} in (8) and (9), we have the following corollary.

Corollary 1: Given (M^l, M^u, V^u) and initial condition x_0, $T_f^{max} \leq T_s^{max}$ for all $D_t \in W$.

Corollary1 indicates that to show $T_f^{max} < \infty$, it suffices to show $T_s^{max} < \infty$, i.e., if the sump state γ_s is less than the allowable lower bound, the donor state γ_d must be less than the allowable lower bound. It is worth noting that in the system dynamics of (1), the toner mass state $M_t(t)$ and the sump state $\gamma_s(t)$ are not explicitly affected by the donor state $\gamma_d(t)$ (shown in Figure 7). This observation together with claim 1 allows us to show $T_f^{max} < \infty$ by showing $T_s^{max} < \infty$, while the later argument can be accomplished by working with toner mass state $M_t(t)$ and sump state $\gamma_s(t)$ only. From now on, we only focus on the first two equations in (1), although the non-negative control input $D_t(t)$ can still depends on all three states. To facilitate our proof, two sets can be defined in the M_t-γ_s phase plane:

$$X_{eq}(C_t) := \left\{ (M_t \geq 0, \gamma_s \geq 0) \;\middle|\; \begin{matrix} (C_t + \dfrac{\beta}{1+p_a} \cdot M_t)\gamma_s = C_t \\ M^l \leq M_t \leq M^u \end{matrix} \right\}, \qquad (10)$$

$$\Delta(M^l, M^u, V^u) := \left\{ (M_t \geq 0, \gamma_s \geq 0) \;\middle|\; \begin{matrix} \gamma_{\min}(M_t, V_{dev}^u, RH) \leq \gamma_s \leq 1 \\ M^l \leq M_t \leq M^u \end{matrix} \right\}. \qquad (11)$$

And a non-intersecting relationship between these two sets can be summarized by the following claim.

Claim 2: Assuming zero waste rate (R_w=0) and a constant throughput rate $C_t \geq 0$, with two subsets defined in (10) and (11), if $\gamma_s < \gamma_{min}$ (defined in (5)) holds for all $(M_t, \gamma_s) \in X_{eq}$, then $\Delta \cap X_{eq} = \Phi$.

Proof:

The equilibrium of the M_t and the γ_s dynamics has zero time derivatives in (1), i.e.

$$0 = D_t(t) - C_t(t)$$

$$0 = \frac{D_t(t)}{M_t(t)}(1+p_a)(1-\gamma_s(t)) - \beta \cdot \gamma_s(t) .$$

Canceling the $D_t(t)$ term in above equations, the equilibrium can be shown to satisfy the equality constraint in (10). Therefore, if $\gamma_s < \gamma_{min}$ holds on $X_{eq}(C_t)$, then $\Delta \cap X_{eq} = \Phi$.

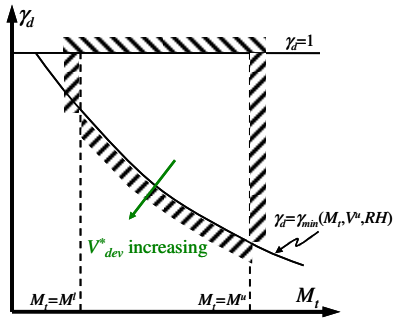

Fig. 5. Projected acceptable operating region in the M_t-γ_d phase plane.

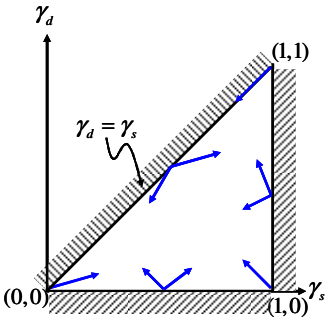

Fig. 6. Positively invariant set $\{0 \leq \gamma_d \leq \gamma_s \leq 1\}$

Remark 2: By definition, X_{eq} is a superset of closed-loop equilibrium. Although for different control input strategies, equilibrium states may change, they will still fall into $X_{eq}(C_t)$, which is valid for all D_t, including all $D_t \in W$. And Δ can be appreciated as follows: The statement that the projection of (3-dimentional) state trajectory onto M_t-γ_s phase plane stays in Δ forever is equivalent to the statement that $T_s^{max} < \infty$. Therefore, claim 2 is a sufficient condition for the non-existence of equilibrium of the reduced dynamics in Δ.

Remark 3: It is also interesting to note that for all $C_t > 0$ the set X_{eq} defined in (10) is a branch of a hyperbola represented by $(1+K_e M_t)\gamma_s = 1$, where $K_e = \beta/[(1+p_a)C_t]$. The location of X_{eq} in the M_t-γ_s phase plane is therefore determined by the developer material property (β and p_a) and throughput rate (C_t). As C_t decreases, X_{eq} shifts down to approach the M_t-axis

as shown in Figure 8. Therefore, for lower throughput rate, $\Delta \cap X_{eq}=\Phi$ is more likely to be satisfied as shown in Figure 8.

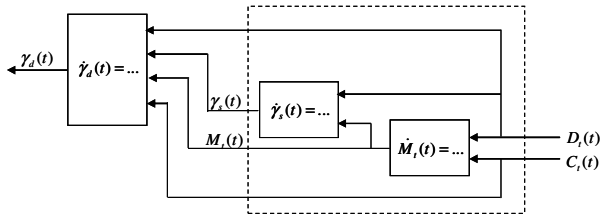

Fig. 7. Structure of the toner aging dynamics

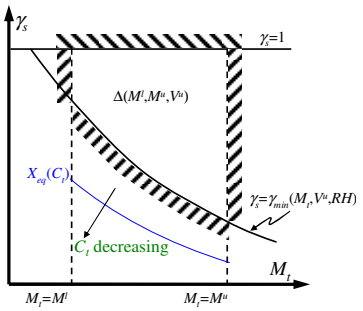

Fig. 8. $X_{eq}(C_t)$ and $\Delta(M^l,M^u,V^u)$

With the invariant property of claim 1 and the equilibrium property of claim 2, the "finite time escaping" property of the dynamics of (1) can be summarized by the following theorem.

Theorem: Assuming zero waste rate (R_w= 0) and the closed-loop system is locally Lipschitz continuous, for any constant throughput rate $C_t \geq 0$, with X_{eq} and Δ defined in (10) and (11), if $\gamma_s<\gamma_{min}$ for all $(M_t,\gamma_s)\in X_{eq}(C_t)$, then for any $D_t \in W$ $T_f^{max}<\infty$ holds.

Remark 4: For any $C_t \geq 0$, by checking the property of the M_t and γ_s dynamics on a superset of closed-loop equilibrium, this theorem gives a sufficient condition for the "finite time escaping" of the three-state dynamics modeled in (1). Detailed proof of this theorem can be found in the Appendix.

Remark 5: As a validation example of the Theorem, D_t has been traditionally adjusted to maintain constant M_t. A direct result of this strategy is that the donor state γ_d keeps decreasing and monotonically increasing V_{dev} is required to maintain *DMA* at its target value *DMA**. When V_{dev} reaches its maximal allowable value V^u at time T_f (~ 9min as shown in Figure 9), the system needs to be adjusted, and otherwise *DMA* can not be maintained at its target values anymore. This matches experimental observations.

4. CONCLUSIONS

In this paper, a hybrid two-component development process has been presented that illustrates the benefit and utility of a control oriented model in system analysis. For the process model and operating conditions under consideration, acceptable operating region analyses have indicated that the loss of developability is a direct result of low throughput rate and therefore the saturation of development voltage is unavoidable for all continuous state feedback involving dispensing strategies. Given the inherent system limitations revealed by the analyses, finding an optimal dispensing strategy to maximize the operating time is one direction of future research.

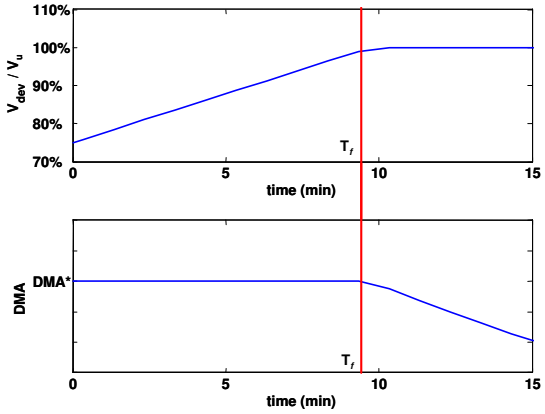

Fig. 9. Simulation results of finite escaping

APPENDIX: PROOF OF THE THEROM

Since $T_f^{max} \leq T_s^{max}$ (corollary1), for the theorem to hold, it suffices to show $T_s^{max}<\infty$ using the M_t and γ_s dynamics. With the assumption that the closed-loop dynamics is locally Lipschitz continuous, the existence and uniqueness of the solution can be guaranteed.

The proof will use the concept of *nonwandering point* and *nonwandering set* for the closed-loop 3-state autonomous system. A point p is called nonwandering with respect to the system dynamics, if for any neighborhood U of p, and any $\tau>0$, there exists a $t>\tau$, such that $\phi(t,U)\cap U \neq \Phi$, where $\phi(t,y)$ denotes the state trajectory at time t with initial condition y, i.e. $\phi(0,y)=y$, and $\phi(t, U)$ denotes all state trajectories starting in U. The set of all such nonwandering points forms the nonwandering set. It can also be shown that if the state trajectory is bounded, the non-wandering set is a compact, nonempty and invariant set (Peterson 1983).

For each point $(M_t,\gamma_s)\in\Delta$ in the M_t-γ_s phase plane, the direction of the (closed-loop) state trajectory is determined by the dispensing $D_t(t)$. A local (may translate along the trajectory) four-quadrant coordinate and a (state and dispensing dependent) tangent angle of trajectory $\theta \in (-\pi, \pi]$ can be defined as in Figure A1

$$\theta(M_t(t),\gamma_s(t),D_t(t)) := \begin{cases} \tan^{-1}\left(\frac{\dot{\gamma}_s}{\dot{M}_t}\right) & \text{in quad. I and IV } (\theta\in[-\pi/2,\pi/2]) \\ \pi-\tan^{-1}\left(\frac{\dot{\gamma}_s}{\dot{M}_t}\right) & \text{in quad. II } (\theta\in(\pi/2,\pi]) \\ \tan^{-1}\left(\frac{\dot{\gamma}_s}{\dot{M}_t}\right)-\pi & \text{in quad. III } (\theta\in(-\pi,-\pi/2)) \end{cases} . \quad \text{(A1)}$$

The slope of the state trajectory can be defined as

$$K := \tan(\theta) = \frac{\dot{\gamma}_s}{\dot{M}_t} = \frac{(1+p_a)(1-\gamma_s)D_t/M_t-\beta\cdot\gamma_s}{D_t-C_t} . \quad \text{(A2)}$$

Note that the so defined slope in (A2) is a monotonic increasing function of the dispensing rate D_t, since

$$\frac{dK}{dD_t} = \frac{-(1+p_a)(1-\gamma_s)C_t/M_t+\beta\cdot\gamma_s}{(D_t-C_t)^2} > 0 , \quad \text{(A3)}$$

for all $D_t \neq C_t$, (when D_t changes from C_t-ε to C_t+ε for some small $\varepsilon>0$, θ changes from -π/2-δ to -π/2+δ for some small $\delta>0$). Therefore, for each point in the projected operating

region, the maximal θ (over all $D_t \geq 0$) can be derived as

$$\theta_{\max}(M_t, \gamma_s) = \tan^{-1}(K)\Big|_{D_t \to \infty} = \tan^{-1}\left[\frac{(1+p_a)(1-\gamma_s)}{M_t}\right] \leq \tan^{-1}\left[\frac{2}{M_t}\right]. \quad \text{(A4)}$$

And the minimal θ (over all $D_t \geq 0$) can be derived as

$$\theta_{\min}(\gamma_s) = \tan^{-1}(K)\Big|_{D_t=0} - \pi = \tan^{-1}(\frac{\gamma_s \beta}{C_t}) - \pi < 0 \quad \text{(A5)}$$

Combining (10-11) with θ_{max} and θ_{min} derived above, we have

$$\theta_{\max} - \theta_{\min} < \pi. \quad \text{(A6)}$$

Equations (A4)-(A6) indicates that for the state trajectory of the closed-loop dynamics to remain in Ω, the following two conditions need to be satisfied simultaneously in the M_t-γ_s phase plane:

(C1). θ_{max}-θ_{min}<π,

(C2). $\theta \notin [\pi/2, \pi]$.

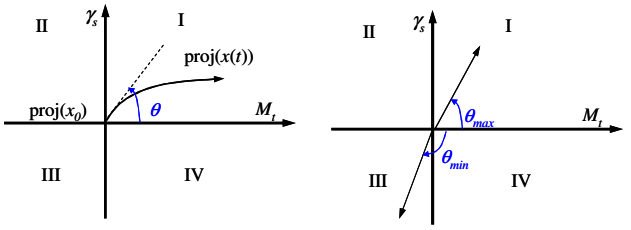

Fig. A1. Local quadrants and tangent angle in the projected operating region.

With these preliminary results, the theorem can be proved with contradiction as shown in Figure A2. Assume that $T_s^{max}=\infty$, an equivalent statement is that $\phi(t,x_0) \subseteq \Omega$ for some initial condition and all $t \geq 0$. Since Ω is compact, $\phi(t, x_0) \subseteq \Omega$ is bounded, a nonwandering point $p \in \Omega$ exists (Peterson 1983), note it is possible that $p \notin \phi(t, x_0)$. Since p is not an equilibrium (by claim 2), there exists a $\varepsilon_p>0$ and a $t_p>0$, such that $|\phi(t_p,p)-p| \geq \varepsilon_p$. However, since p is an nonwandering point, if we chose its neighborhood U as $U:=B(p,\varepsilon_p/M)$, where $M>>1$, i.e. an open ball centered at p with a much smaller radius and we chose $\tau=t_p$, according to the definition of nonwandering point, a $t^*>\tau$ exists, such that $\phi(t^*,U) \cap U \neq \Phi$, in particular, there exists a $p_1 \in U$, such that $|\phi(t^*,p_1)-p| < \varepsilon_p/M$, i.e., the state trajectory starting from p_1 will return to the much smaller ball $B(p,\varepsilon_p/M)$ after leaving $B(p,\varepsilon_p)$. If we denote $p_2=\phi(t^*,p_1)$, we can show that $|p_2-p_1| < 2\varepsilon_p/M$, i.e. the projection of state trajectory $\phi(t,p_1)$, $t \in [0, t^*]$ onto phase plane is almost a closed curve M_t-γ_s. Since $B(p,\varepsilon_p/M)$ can be made as small as we wish, the state trajectory can be made arbitrarily close to a closed curve in the M_t-γ_s phase plane, therefore the velocity constraints at p_2 can be made arbitrarily close to those at p_1. However, when traveling along an "almost closed" curve, the tangent angle changes from -π to π continuously, thus C2 is violated. The proof is complete.

Remark A1: Note that in this proof, it is assumed that the projection of the state trajectory does not intersect with itself on the M_t-γ_s phase plane, if intersection happens (possible due to the γ_d dependent input), the above argument can be applied to the point of intersection. Another remark here is although condition C1 is not explicitly used in the proof, it is necessary in the sense that it rules out the case where the trajectory returns along the leaving path. The last remark about this proof is that since the input also depends on γ_d, theorems for two-state dynamics (Poincare-Bendixson theorem etc.) can not be applied directly.

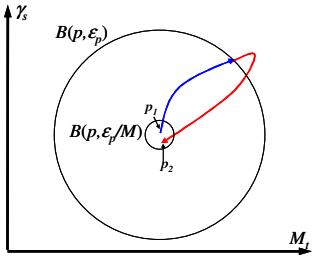

Fig. A2. Projection of an "almost" closed trajectory onto the M_t-γ_s phase plane.

REFERENCES

Blanchini, F. (1999). Set invariance in control, *Automatica*, **Vol. 35**, pp. 1747-1767.

Grasselli, O. M. and Isidori, A. (1981). An existence theorem for observers of bilinear systems. *IEEE Trans. Automatic Control*, **Vol 26**, pp. 1299-1230.

Hirsch, M. (2006). Is image-on-image color printing a privileged printing architecture for production digital printing applications?. *Proceedings of the IS&T's NIP20: International Conference on Digital Printing Technologies*, **Vol 22**, pp. 398–401.

Khalil, H. K. (2002). *Nonlinear Systems,* 3rd Edition. Prentice Hall, New Jersey.

Li, P. and Dianat, S. (2001). Robust stabilization of tone reproduction curves for the xerographic printing process. *IEEE Trans. Control Systems Technology*, **Vol 9**, pp. 407-415.

Liebman, A. J. (1975). Toner loading for touchdown donor, *U.S. Patent,* 3,929,098.

Liu, F., Chiu, G. T.-C., Hamby, E. S., Eun, Y. and Ramesh, P. (2006a). Control oriented modeling of a hybrid two-component development process for xerography. *Proceedings of the IS&T's ICIS06: International Congress of Image Science*, pp. 87–90.

Liu, F., Chiu G. T.-C., Hamby E. S. and Eun Y. (2006b). Control analysis of a hybrid two-component development process. *Proceedings of the IS&T's NIP22: International Conference on Digital Printing Technologies*, **Vol 22**, pp. 564–567.

Nijmeijer, H. and Schaft, A. V. (1982). Controlled Invariance for Nonlinear Systems. *IEEE Trans. Automatic Control*, **Vol. AC-27**, No. 4, pp. 904-914.

Pai, D.M. and Springett, B. (1993). Physics of electrophotography. *Reviews of Modern Physics*, **Vol 65**, pp. 163-211.

Peterson, K. (1983), *Ergodic Theory*, University Press, Cambridge.

Ramesh, P. (2005), Quantification of toner aging in two component Development Systems. *Proceedings of the IS&T's NIP21: International Conference on Digital Printing Technologies*, **Vol 21**, pp. 544–547.

Shein, L.B. (1988). *Electrophotography and development physics*. Springer-Verlag, New York.